

pubs.acs.org/JCTC Article

Cooperativity and Frustration Effects (or Lack Thereof) in Polarizable and Non-polarizable Force Fields

Jorge Nochebuena, Jean-Philip Piquemal, Shubin Liu, and G. Andrés Cisneros*



Cite This: J. Chem. Theory Comput. 2023, 19, 7715-7730



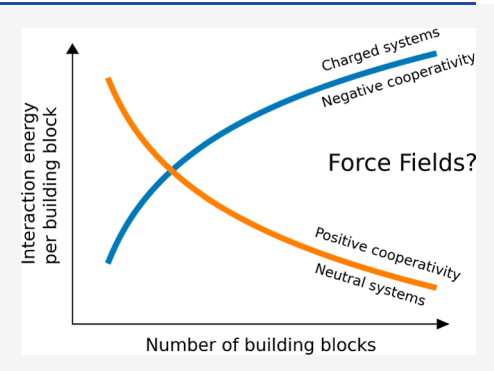
ACCESS

III Metrics & More

Article Recommendations

Supporting Information

ABSTRACT: Understanding cooperativity and frustration is crucial for studying biological processes such as molecular recognition and protein aggregation. Force fields have been extensively utilized to explore cooperativity in the formation of protein secondary structures and self-assembled systems. Multiple studies have demonstrated that polarizable force fields provide more accurate descriptions of this phenomenon compared to fixed-charge pairwise nonpolarizable force fields, thanks to the incorporation of polarization effects. In this study, we assess the performance of the AMOEBA polarizable force field and the AMBER and OPLS nonpolarizable pairwise force fields in capturing positive and negative cooperativity recently explored in neutral and charged molecular clusters using density functional theory. Our findings show that polarizable and nonpolarizable force fields qualitatively reproduce the relative cooperativity observed in electron structure calculations. However,



AMBER and OPLS fail to describe absolute cooperativity. In contrast, AMOEBA accounts for the absolute cooperativity by considering interactions beyond pairwise interactions. According to the energy decomposition analysis, it is observed that the electrostatic interactions calculated with the AMBER and OPLS force fields seem to play an important and counterintuitive role in reproducing the adiabatic interaction energies calculated with density functional theory. However, it is important to note that these force fields, due to their nature, do not explicitly incorporate many-body effects, which limits their ability to accurately describe cooperativity. On the other hand, frustration in polarizable and nonpolarizable force fields is caused by changes in bond stretching and angle bending terms of the building blocks when they are forming a complex.

INTRODUCTION

Cooperativity plays a crucial role in understanding various biological processes, including molecular recognition, homochirality, protein folding, and self-assembly. $^{1-11}$ Cooperativity refers to the nonadditive and synergistic effects that arise when multiple components interact, leading to enhanced stability or activity. One of the most well-known examples of cooperativity is the binding of aqueous O_2 to hemoglobin. When one of the four binding sites of hemoglobin binds an oxygen molecule, it triggers a conformational change that makes it easier for the other sites to bind oxygen as well.

Positive (negative) cooperativity occurs when the interactions between components of a system favor (disfavor) each other. By contrast, no cooperativity is observed when the interactions of the entire system can be represented by the individual interactions of its components. Conversely, frustration refers to the situation in which the optimal geometric arrangement of a set of isolated molecules changes upon the formation of a new molecular system. This change in geometry can result from the intermolecular interactions and bonding between the molecules, which can lead to a deviation of individual molecular geometries from the optimized gas phase structure. This suboptimal arrangement is referred to as frustration, as it deviates from the ideal or expected geometric arrangement. Cooperativity and frustration are two inter-

connected concepts, each emphasizing different aspects. Cooperativity primarily examines the behavior of systems as a whole, while frustration delves into the characteristics of individual components.¹²

Force fields have been used as a tool for investigating cooperative effects involved in the formation of protein secondary structures and self-assembled systems. ^{13–15} Notably, a growing body of evidence supports the superiority of polarizable force fields over fixed-charge force fields in providing more accurate descriptions of cooperativity due to the (partial) incorporation of terms that are explicitly involved in many-body effects. ^{16–19} By explicitly incorporating the concept of polarization effects, polarizable force fields can simulate for the dynamic electronic redistribution that occurs within molecular systems. ^{20,21} In contrast, fixed-charge force fields neglect the dynamic nature of charge distributions that arise from polarization and charge transfer interactions. ²²

Received: July 11, 2023
Revised: September 5, 2023
Accepted: October 12, 2023
Published: October 27, 2023





In this work, we focus on studying cooperativity and frustration using molecular mechanics to evaluate the capability of force fields to reproduce these effects. We used three representatives: $NH_3(H_2O)_n$, $Li^+(H_2O)_n$, and $F^-(H_2O)_n$ for neutral and charged systems. The previous systems have been studied using density functional theory. 23-26 Positive cooperative effects were observed in neutral systems, and negative cooperativity was observed in charged systems. On the other hand, it was shown that the frustration effect is smaller than cooperativity and can be positive or negative. Previously, some of us have shown that the cooperativity of hydrogen bonds in infinite linear chains can be modeled using point dipoles.²⁷ Therefore, it is of interest to investigate whether force fields can reproduce these effects in molecular clusters, since these effects play a significant role for the accurate calculation of various thermodynamics and transport properties such as solvation-free energy, diffusion, residence time, etc. Some of these properties have been studied computationally for similar systems previously via Born–Oppenheimer QM/MM MD. $^{28-30}$

■ THEORETICAL FRAMEWORK

We used molecular systems of the form AB_n , where B is the building block, n is the number of building blocks, and A is the accessory component to quantify both cooperativity and frustrativity. In this work, water molecules are the building blocks, and NH_3 , Li^+ , and F^- are the accessory components.

To calculate cooperativity and frustrativity, we need to calculate the adiabatic and vertical interaction energies. The adiabatic interaction energy (AIE) is defined as

$$E_{\text{int}}^{\text{adiab}} = E(AB_n) - nE_B(R_{0B}) - E_A(R_{0A})$$
 (1)

where n is the number of building blocks included in the system, E is the total energy of the whole system, $E_{\rm B}$ is the total energy of the building block with the optimized structure $R_{\rm 0B}$, and $E_{\rm A}$ is the total energy of the accessory component with the optimized structure $R_{\rm 0A}$.

The cooperativity index k is defined as the negative change of AIE per building block change, that is

$$k = -(\partial E_n/\partial n) \tag{2}$$

where E_n is the interaction energy per building block obtained by dividing the AIE by the number of building blocks, that is

$$E_n = E_{\rm int}^{\rm adiab}/n \tag{3}$$

The parameter k can have three possible scenarios. If k is positive, the cooperativity is positive, and it means that adding an additional building block makes the interactions stronger. If k is negative, then cooperativity is negative, and it means that adding a building block weakens the interactions. Otherwise, if k is zero, there is no cooperativity, and it means that adding an additional building block has no impact on the interactions.

The vertical interaction energy (VIE) is defined as

$$E_{\text{int}}^{\text{vert}} = E(AB_n) - \sum_{B=1}^{n} E_B(R_B) - E_A(R_A)$$
 (4)

where $E_{\rm B}$ is the total energy of each building block with structure $R_{\rm B}$, and $E_{\rm A}$ is the total energy of the accessory component with the structure $R_{\rm A}$.

Note that the difference between eqs 1 and 4 depends on which molecular geometry is used in each case. In eq 1 the

optimized geometries of the individual molecules are used, while in eq 4 the geometries of the molecules forming the system are used. Because molecules outside of their optimized gas-phase geometry will always have a higher energy than their corresponding equilibrium structures, the VIE will always be more stabilizing than the AIE.

Then, the total frustration energy (FE) can be defined as the difference between the AIE and the VIE; that is

$$E_{\text{frust}} = \sum_{B=1}^{n} E_{B}(R_{B}) + E_{A}(R_{A}) - nE_{B}(R_{0B}) - E_{A}(R_{0A})$$
(5)

In a similar way to cooperativity, the frustration per building block can be defined as

$$E_{0n} = E_{\text{frust}}/n \tag{6}$$

and frustrativity as

$$\zeta = \partial E_{0n} / \partial n \tag{7}$$

If ζ is positive, then frustrativity is positive and means that adding an additional building block increases the difference in geometry of the individual molecules when they are part of the system. If ζ is negative, frustrativity is negative and means that adding a new building block reduces the geometric difference between the individual molecules and forms the system. If ζ is zero, frustrativity is zero, and it means that adding a new building block does not affect the geometry of the individual molecules.

We refer to the previous form of measuring of cooperativity as relative cooperativity because estimating the value of cooperativity for a given number of building blocks, n, requires knowing the interaction energy of a smaller cluster (n-1) and a larger cluster (n+1).

In addition, we are also interested in investigating how force fields reproduce absolute cooperativity. As described above, cooperativity is exclusively due to many-body effects. Therefore, an important question is how force fields can model some cooperativity effects. In particular, it is known that, by construction, pairwise nonpolarizable potentials do not explicitly include many-body effects. One possibility is to determine if the following condition is satisfied

$$E_{\text{int}}^{\text{vert}} = \sum_{B=1}^{n} [E_{AB} - E_B - E_A] + \sum_{B=1}^{n-1} \sum_{C=B+1}^{n} [E_{BC} - E_B - E_C]$$
(8)

where AB is a dimer formed by the accessory component, A, and a building block, B, and BC is a dimer formed by the building blocks B and C. If eq 8 is satisfied, it means that the VIE can be represented through individual interactions, and therefore there is no cooperativity. On the other hand, if the VIE is more stabilizing than the right-hand side of eq 8, it means there is an energy gain and thus positive absolute cooperativity. Conversely, if the VIE is less stabilizing than the right-hand side of eq 8, it means there is an energy loss due to the formation of the complex and therefore negative absolute cooperativity.

COMPUTATIONAL DETAILS

In this work, we calculated the relative cooperativity, eq 2, and the frustrativity, eq 7, in three representative molecular

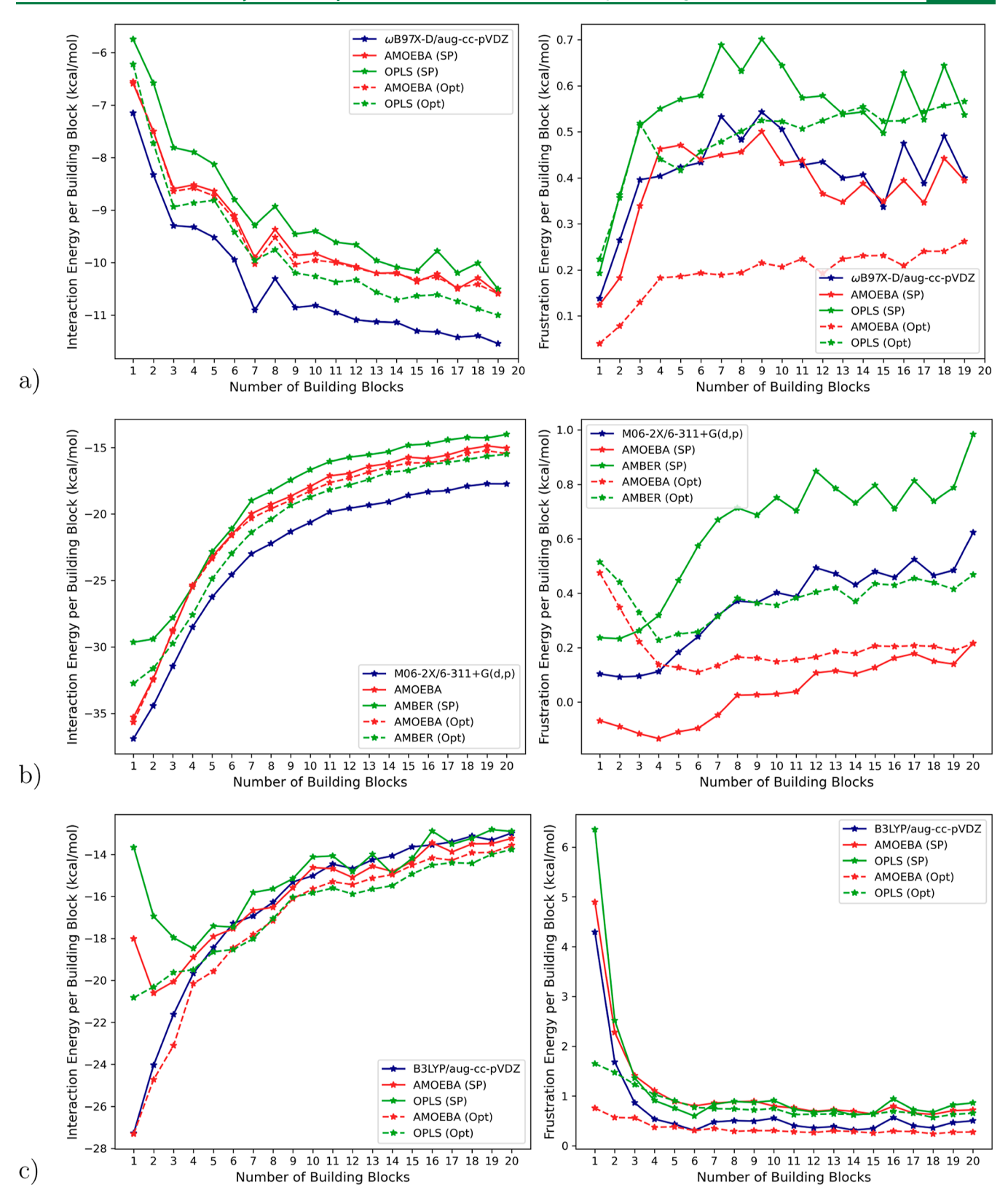


Figure 1. Relative cooperativity (left) and frustrativity (right) for (a) $NH_3(H_2O)_n$, (b) $Li^+(H_2O)_n$, and (c) $F^-(H_2O)_n$ systems. Solid lines are single-point values calculated from optimized DFT structures, while dashed lines are calculated in optimized FF structures.

systems: an ammonia molecule in water, $NH_3(H_2O)_n$, a lithium cation in water, $Li^+(H_2O)_n$, and a fluorine anion in water, $F^-(H_2O)_n$. The first of these systems is a neutral system, while the last two are positively and negatively charged

systems, respectively. In all cases, systems from 1 to 20 building blocks were considered.

The optimized DFT molecular geometries were taken from the work of Liu and Rong.²⁶ Each system has the global

minimum for each number of building blocks. We optimized a water molecule as a building block and the accessory components with density functional theory using Gaussian16. The exchange–correlation functionals and basis sets correspond to those used by Liu and Rong, hamley ω B97X-D/aug-cc-pVDZ for NH₃(H₂O)_n, hole-2X/6-311+G(d,p) for Li⁺(H₂O)_n, hole-2X/6-311+G(d,p) hole-2X/6-311+G(d,p) for Li⁺(H₂O)_n, hole-2X/6-311+G(d,p) hole-2X

To evaluate the performance of force fields in reproducing previously reported results with DFT, we considered two scenarios: in the first scenario, we performed single-point calculations on each of the systems optimized with DFT. In the second scenario, we carried out optimization of the systems with force fields using Tinker8 to calculate the adiabatic and vertical interaction energies. Water molecules are described with the AMOEBA and TIP3P parameters by using polarizable and nonpolarizable force fields, respectively. In particular, we used the flexible TIP3P model implemented in Tinker, with an O–H bond stretching force constant of 553.0 and 600 kcal/mol/Ų, and an H–O–H angle bending force constant of 100.0 and 75.0 kcal/mol/rad², for the Amber and OPLS force fields, respectively. So

To evaluate whether eq 8 was satisfied, we computed vertical interaction energies for each possible dimer within the first four clusters $(1 \le n \le 4)$ for each of the systems studied here. We then performed single-point calculations using the same levels of theory described earlier, using the Psi4 code, and compared them with the equivalent systems calculated with force fields. In addition, we utilized the symmetry-adapted perturbation theory within density functional theory, SAPT-(DFT), implemented in Psi4 to analyze the noncovalent interaction components in these systems.

■ RESULTS AND DISCUSSION

We evaluated relative cooperativity and frustrativity in three representative neutral and charged systems: NH₃(H₂O)₁₁,

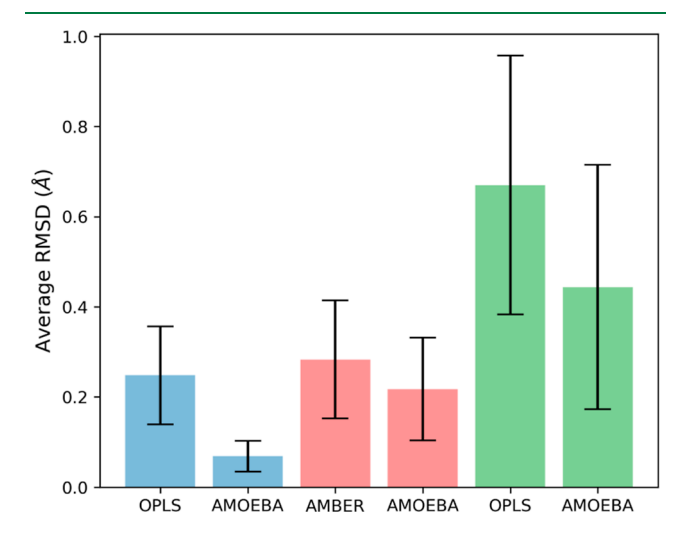


Figure 2. Average root-mean-square deviation (RMSD) between DFT and force field coordinates for the for (a) $NH_3(H_2O)_n$, (b) $Li^+(H_2O)_n$, and (c) $F^-(H_2O)_n$ systems shown in blue, red, and green bars, respectively. Error bars indicate the standard deviation.

 $Li^{+}(H_2O)_n$, and $F^{-}(H_2O)_n$. We selected these systems because the parameters of the force fields already existed to describe each molecule of the systems. As previously mentioned, cooperativity is a phenomenon that cannot be captured by pairwise contributions alone because it involves complex many-body interactions. Knowing that force fields such as AMBER and OPLS lack many-body interactions, we examine the capability of force fields to reproduce the adiabatic interaction energies using clusters of varying sizes. Tables S1-S6 shows the total adiabatic and vertical interaction energies for each of the systems studied in this work. Tables S1, S3, and S5 show the interaction energies calculated via a single point on the structures optimized with DFT. Conversely, Tables S2, S4, and S6 show the interaction energies using the structures optimized with their respective force fields. Each row indicates the interaction energy for each number of building blocks calculated with density functional theory and polarizable and nonpolarizable force fields.

As expected, the vertical interaction energies are more negative than the adiabatic interaction energies for almost all cases due to the effect of considering the total energy of each molecule in its optimized gas-phase configuration or not. For the systems corresponding to the optimized DFT structures (Table S3) to calculate the interaction energies of the Li⁺(H₂O), system with AMOEBA, the first seven values exhibit an opposite trend, that is, the AIE is more stabilizing than the VIE. This can be explained because we do not allow the geometry to be optimized for the force field used. That is, the optimizations made with density functional theory do not necessarily coincide with the optimized structure for the force field. For example, the optimal H-O-H angle in a water molecule calculated with AMOEBA is 108.5°, but the same angle calculated using any of previous exchange-correlation functionals ranges between 104.8 and 105.2°. However, when we allow the system to relax (Table S4), the expected behavior is obtained.

We also note that for the $\mathrm{NH_3(H_2O)}_n$ and $\mathrm{Li}^+(\mathrm{H_2O})_n$ systems, the interaction energies obtained with the exchange—correlation functionals show more negative values than the force fields. On the other hand, for the $\mathrm{F}^-(\mathrm{H_2O})_n$ system, the lowest interaction energies were obtained with the force fields. This could be due to the different types of functionals and force fields used in each case. However, in all cases, we can see that the force fields reproduce the same trends obtained with density functional theory

Figure 1 shows the cooperativity and frustrativity profiles for the systems studied in this work. It shows the values obtained for the force fields using optimized DFT geometries and the values obtained for the force fields with their respective optimized structures. The values shown correspond to the energies of interaction and frustration for each building block. As previously reported, the $NH_3(H_2O)_n$ (neutral) system shows positive cooperativity in that as the number of building blocks increases, the interaction energy per building block also increases, using either DFT or force fields. We can see that the largest building block interaction energies were obtained with DFT. However, both the OPLS polarizable and the AMOEBA nonpolarizable force field reproduce the behavior of DFT, although the interaction energies are lower. Frustrativity is positive whether using DFT or force fields. That is, in all cases, the cooperativity and frustrativity are positive. In Figure 1a, we can see that the optimization of the structures improves the

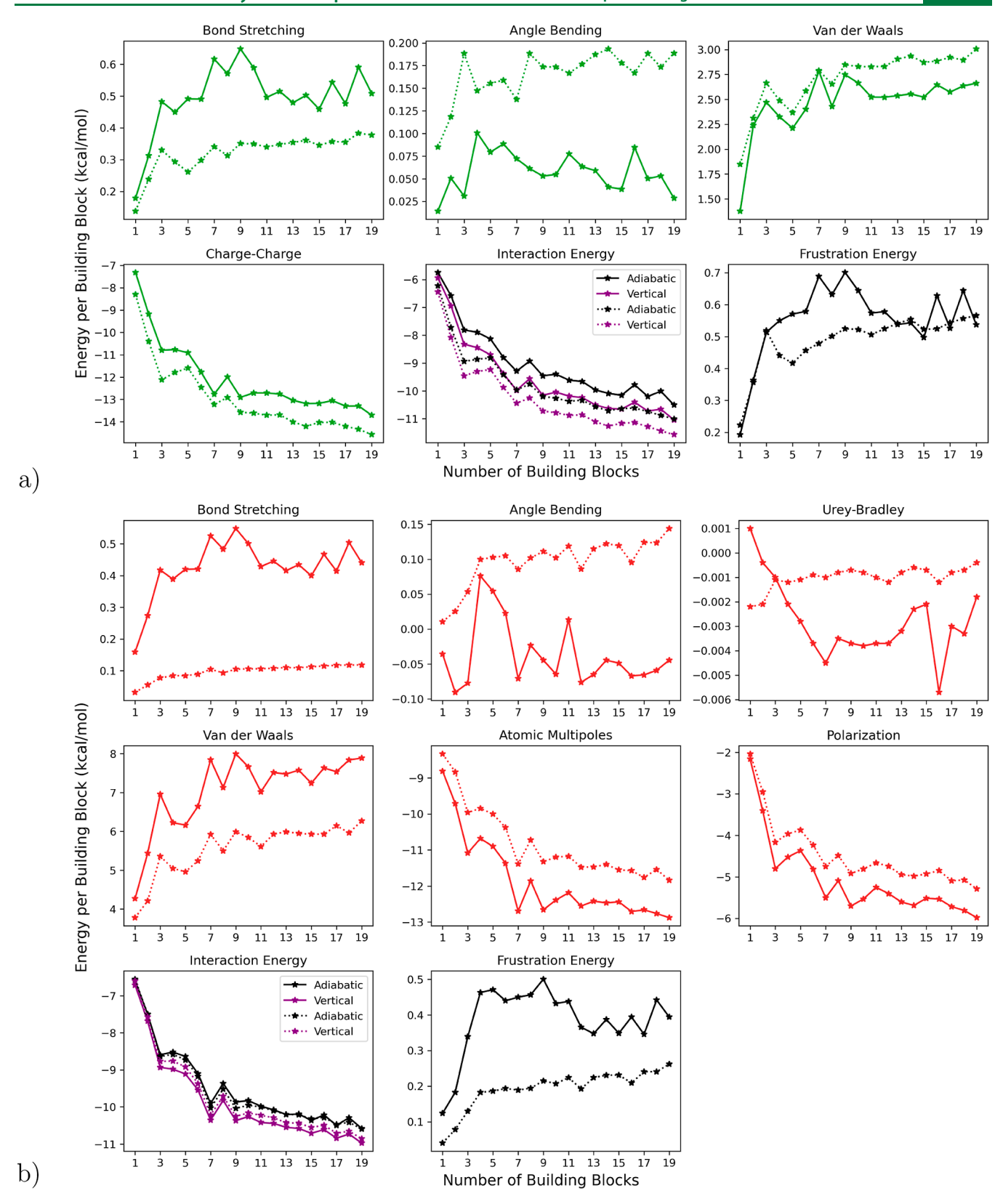


Figure 3. Energy decomposition analysis for the $NH_3(H_2O)_n$ system. (a) OPLS, (b) AMOEBA. Solid lines represent single point values calculated from optimized DFT structures, while the dotted line values were calculated using optimized FF structures.

description of the interaction energy, especially with the OPLS force field. However, the FE undergoes several changes, increasing the difference with the results reported with DFT.

As previously reported, $\operatorname{Li}^+(H_2O)_n$ and $\operatorname{F}^-(H_2O)_n$ (charged systems) show negative cooperativity since, as the size of the system increases, the interaction energy per building block decreases. Considering the structures not optimized by force

Table 1. Correlation Coefficients between Each of the Contributions and the AIE, VIE, and FE for the NH₃(H₂O), System

		AIE		V	TE	FE		
		DFT ^a	FF^b	DFT^c	FF^d	DFT^e	FF^{b}	
OPLS	bonds	-0.722	-0.965	-0.762	-0.969	0.984	0.985	
	angles	-0.113	-0.843	-0.151	-0.851	0.526	0.933	
	vdW	-0.821	-0.980	-0.845	-0.982	0.861	0.975	
	charges	0.989	0.999	0.995	0.999	-0.768	-0.966	
AMOEBA	bonds	-0.769	-0.993	-0.802	-0.994	0.875	0.961	
	angles	0.232	-0.874	0.185	-0.881	0.419	0.983	
	UB^c	0.702	-0.872	0.728	-0.877	-0.741	0.926	
	vdW	-0.938	-0.983	-0.945	-0.982	0.667	0.913	
	PE^d	0.984	0.995	0.987	0.994	-0.631	-0.926	
	Pol. ^e	0.971	0.986	0.979	0.987	-0.689	-0.947	

[&]quot;Single point values calculated over optimized DFT structures. "Values calculated over optimized FF structures. "Urey—Bradley term. "Permanent electrostatic." Polarization.

fields (Figure 1b), the polarizable and nonpolarizable force fields reproduce quite well the cooperativity obtained by DFT for the $Li^+(H_2O)_n$ system, with the performance for the AMOEBA polarizable force showing slight better agreement, especially for the first two structures. However, the frustration calculated with AMOEBA shows an interesting behavior, since for the first structures, the FE has negative values. This means that the molecules forming the system have lower energies than the isolated molecules. As already discussed above, the reason for this behavior is because the optimized structure of the individual molecules obtained with DFT is different than the optimized structures of AMOEBA. On the other hand, the AMBER nonpolarizable force field better reproduces the frustration, although it is far from the values obtained with DFT. If the optimized structures with the force fields are used (Figure 1b), it can be observed that the interaction energies are in much better agreement with respect to the reference. On the other hand, although frustration shows positive values for both force fields, the results show significant changes that are far from the results obtained with DFT.

For the $F^-(H_2O)_n$ system, we note that both AMOEBA and the OLSAA nonpolarizable force field quite accurately reproduce the frustration calculated with B3LYP when structures not optimized by force fields are used (Figure 1c). However, cooperativity shows interesting behavior. For the first systems, the cooperativity calculated with the force fields shows decreasing values for the first structures, indicating a negative cooperativity. But after the system reaches a certain size, the cooperativity is positive. Here, the OPLS force field is that shows the largest deviations from the reference. When using the geometries optimized by force fields (Figure 1c), the interaction energies closely approximate the reference values. However, frustration becomes more prominent, particularly in smaller systems.

As can be seen in Figures 2, S1–S6 and Table S7, the largest differences in geometric coordinates for the structures optimized with the force fields occur with the nonpolarizable force fields. The $NH_3(H_2O)_n$ system shows the smallest errors, whether using polarizable or nonpolarizable force fields. For this system, the largest RMSD is 0.2 Å when using the AMOEBA force field and 0.45 Å when using the OPLS force field. The $Li^+(H_2O)_n$ system shows a maximum RMSD of 0.4 Å with AMOEBA and a maximum RMSD of 0.65 Å with the AMBER force field. Finally, the $F^-(H_2O)_n$ system shows the

largest deviations, with an RMSD of 0.98 Å for AMOEBA and 1.24 Å for the OPLS force field.

We conducted an energy decomposition analysis of the total potential energy to discern the sources of relative cooperativity and frustrativity obtained using force fields. Understanding how force fields such as AMBER and OPLS can simulate this phenomenon is truly intriguing, particularly considering that cooperativity, as calculated using density functional theory, incorporates contributions from many-body interactions. We did not repeat the analysis for the energies obtained with DFT since it has already been reported previously.²⁵ For the OPLS and AMBER nonpolarizable force fields, the decomposition results in four terms that correspond to bond stretching, angle bending, van der Waals interactions, and charge-charge interactions. For the AMOEBA polarizable force fields, the individual terms correspond to bond stretching, angle bending, Urey-Bradley interactions, van der Waals interactions, permanent electrostatic interactions, and polarization. In both cases, we have included the adiabatic and vertical interaction energies and the FE interaction energy per building block for easy comparison. Solid lines show the values calculated with the optimized structures obtained from the exchange-correlation functionals, and dotted lines show the values obtained using the optimized structures with the force fields used.

Figure 3 shows the energy decomposition analysis for the NH₃(H₂O)_n system calculated with the OPLS and AMOEBA force fields. The results show that the relative cooperativity comes mainly from intermolecular nonbonded electrostatic interactions, that is, from the charge-charge interaction with the OPLS force field and from the polarization and atomic multipoles with the AMOEBA force field, with the permanent electrostatics exhibiting the largest contribution. We can see from Table 1 that the highest correlation between the adiabatic and vertical interaction energies occurs for the electrostatic interaction when using the OPLS force field. Similarly, for the AMOEBA force field, the largest correlation is obtained between permanent electrostatics and polarization. In both cases, similar values are observed in the structures optimized either by the exchange-correlation functional or by the force field. The van der Waals contribution increases as the number of building blocks increases, with the AMOEBA polarizable force field showing van der Waals energy more than two times larger than the same term calculated with the OPLS nonpolarizable force field.

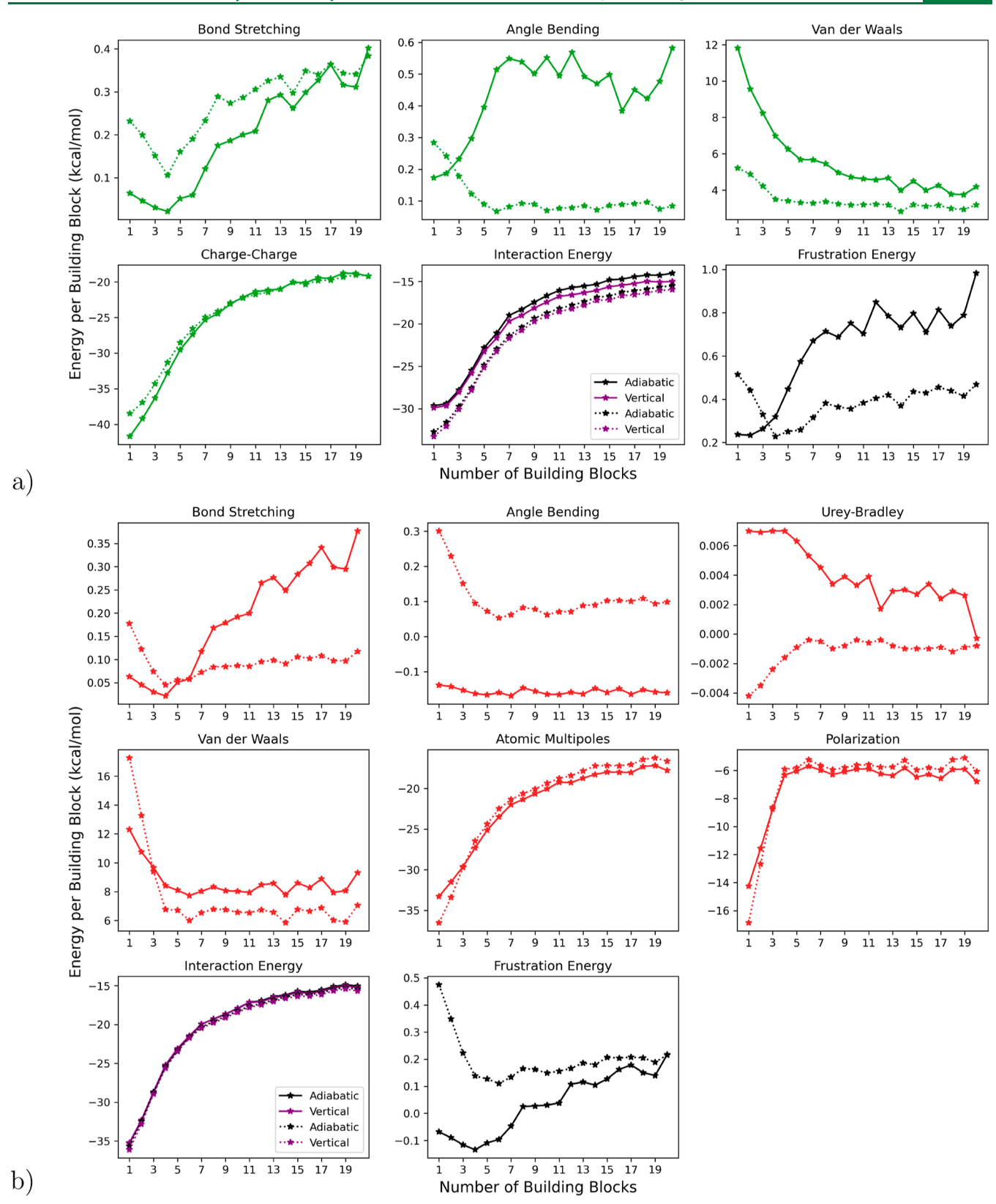


Figure 4. Energy decomposition analysis for the $\text{Li}^+(\text{H}_2\text{O})_n$ system. (a) AMBER, (b) AMOEBA. Solid lines represent single point values calculated from optimized DFT structures, while the dotted line values were calculated using optimized FF structures.

From the same Table 1, we can see that the largest correlation for frustration occurs with respect to the bond stretching term for the structures optimized by the exchange—correlation functional. This can be observed from the shape of

the graph, which is very similar to the FE per building block. Furthermore, the energy range of the bond stretching term is larger by almost an order of magnitude compared to the energy range of the angle bending term. On the other hand, for the

Table 2. Correlation Coefficients between Each of the Contributions and the AIE, VIE, and FE for the Li⁺(H₂O)_n System

		AIE		V	TE	FE		
		DFT ^a	FF^{b}	DFT ^a	FF^b	DFT ^a	FF^{b}	
AMBER	bonds	0.892	0.838	0.890	0.831	0.887	0.718	
	angles	0.823	-0.836	0.819	-0.843	0.889	0.327	
	vdW	-0.949	-0.895	-0.950	-0.901	-0.888	0.215	
	charges	0.995	0.998	0.996	0.999	0.950	0.177	
AMOEBA	bonds	0.834	-0.252	0.828	-0.262	0.997	0.887	
	angles	-0.472	-0.780	-0.478	-0.786	-0.062	0.974	
	UB^c	-0.867	0.867	-0.862	0.872	-0.919	-0.899	
	vdW	-0.768	-0.860	-0.775	-0.865	-0.255	0.930	
	PE^d	0.995	1.000	0.994	1.000	0.843	-0.641	
	Pol. ^e	0.842	0.860	0.848	0.866	0.370	-0.933	

^aSingle point values calculated over optimized DFT structures. ^bValues calculated over optimized FF structures. ^cUrey—Bradley term. ^dPermanent electrostatic. ^ePolarization.

structures optimized with the force field, a significant correlation is observed between the bond stretching and the angle bending terms for both the nonpolarizable and polarizable force fields. In both cases, the optimization decreases the contribution of the bond stretching term but increases the contribution of the angle bending term. The Urey—Bradley contribution when using the polarizable force field does not make a significant contribution for this system.

In Figure 4, we observe that in the case of the ${\rm Li}^+({\rm H_2O})_n$ system, the negative relative cooperativity also comes from the charge—charge interactions with the AMBER force field and from the polarization and permanent electrostatic interactions with AMOEBA, the latter being the one that contributes the most.

From Table 2, we can see that the main correlation between the adiabatic and VIE is obtained with the charge—charge interactions with the AMBER force field and with permanent electrostatics with AMOEBA, either before or after the force field optimization. The van der Waals contributions for the two force fields used are similar for the smaller complexes but decrease in a different way as the number of building blocks increases. In addition, geometry optimization has a different impact on each force field used. The contribution increases with the AMBER force field, while it decreases with AMOEBA, possibly reflecting the difference in the functional form between the two force fields. In AMOEBA, the 14—7 buffered Halgren potential is utilized to describe the van der Waals (vdW) interactions, ⁵¹ whereas OPLS and AMBER use the 6—12 Lennard-Jones (LJ) potential. ^{52–54}

From the same Table 2, we can see that the best correlation for frustration with the AMBER force field is obtained with charge-charge interactions using structures not optimized by the force field. However, this is a fortuitous result since, by definition, the frustration must come from intramolecular changes. On the other hand, it can be seen that both the bond stretching and angle bending terms show similar correlation coefficients for the AMBER force field before optimization with the force field. After optimization, the bulk of the correlation is obtained from the bond stretching term. For AMOEBA, the major contributor to the correlation is obtained from the bond stretching term when DFT-optimized structures are used. Here the angle bending term shows negative results, regardless of the number of building blocks. This result shows that the negative values of frustration previously observed in this system come from the difference of the optimal values of the H–O–H angles between the M06-2X exchange correlation functional and AMOEBA. However, during the optimization process, this behavior is corrected, resulting in positive values for all building blocks. In fact, the primary correlation with frustration is observed in the angle bending term, with the bond stretching term following closely behind. Again, the Urey–Bradley term practically does not contribute to the total energy.

In Figure 5, we can see that once again, the negative relative cooperativity in the $F^-(H_2O)_n$ system comes from the chargecharge interaction with the OPLS force field and from the permanent electrostatics with AMOEBA for the optimized systems. However, when single-point calculations are calculated using the optimized DFT structures, we obtain low correlation coefficients for the AIE (see Table 3). This can be explained because, by contrast to the previous two systems, here we note a significant discrepancy between the adiabatic and vertical interaction energies in systems with few building blocks when using either the OPLS nonpolarizable force field or the AMOEBA polarizable force field. The structural differences between complex-forming molecules and isolated molecules are the primary cause of this disparity. Therefore, if the correlation coefficients are calculated using the VIE, better results are obtained for the OPLS and AMOEBA force field (see Table 3).

Like the previous system, the van der Waals contribution is smaller as the number of building blocks increases. We note that optimization of the structures strongly reduces the contribution of van der Waals forces, especially for systems with the fewest number of building blocks. The results demonstrate that the bond stretching term is the primary cause of the observed frustration compared to the systems calculated with the optimized DFT structures. In systems optimized by force fields, similar correlation coefficients can be observed for both bond stretching and angle bending terms.

To explore whether force fields can replicate absolute cooperativity, which arises from many-body interactions, we calculated the vertical interaction energies in dimers for the first four clusters of each studied system. This analysis aimed to determine whether the force fields adhere to eq 8 or not. For n = 1, only one dimer is possible. As n increases, the number of possible dimers also grows. Specifically, for n = 2, three dimers are possible; for n = 3, there are six possible dimers; and for n = 4, there are ten possible dimers. The results of these vertical interaction energies per dimer are presented in Tables 4-6. In

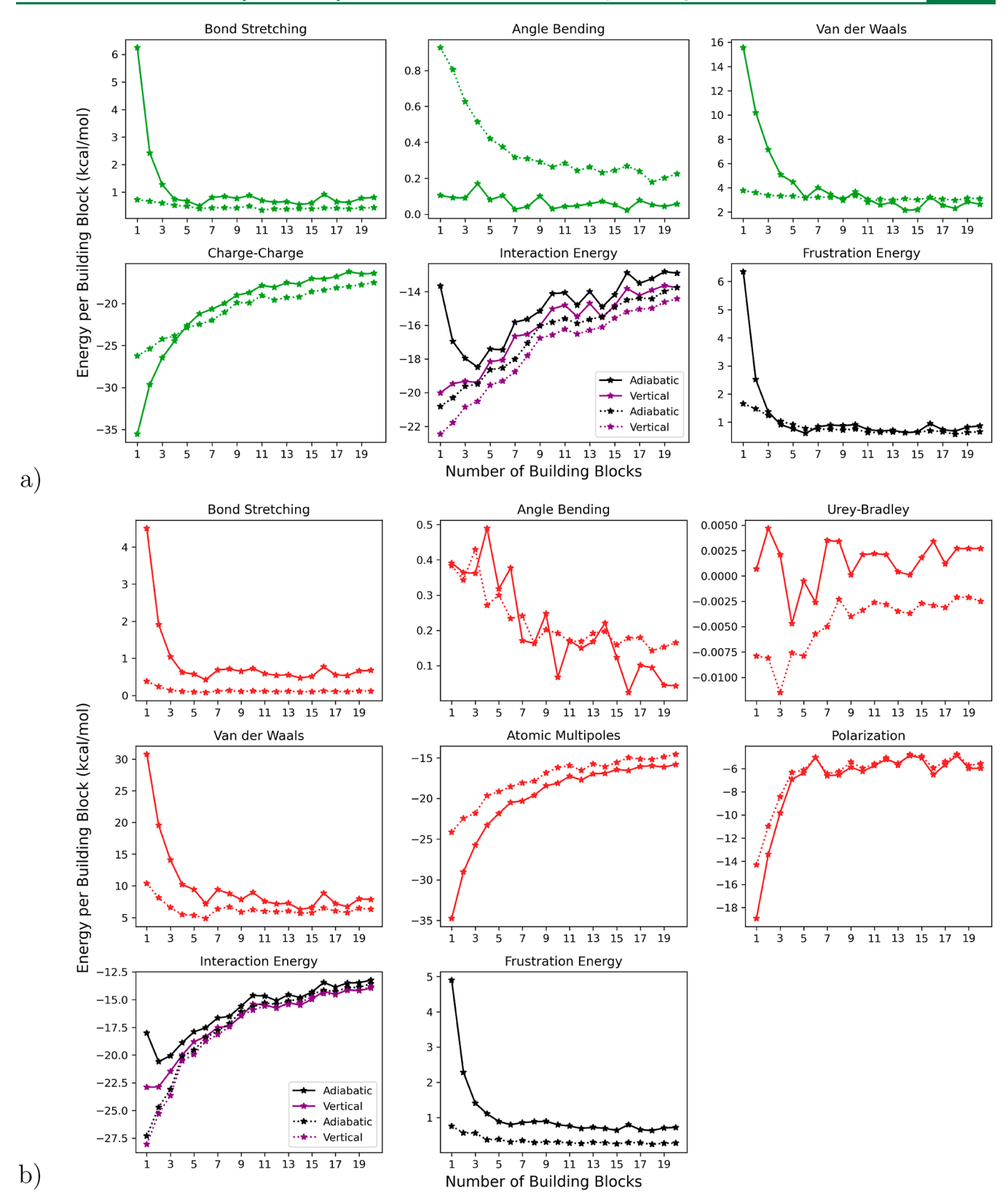


Figure 5. Energy decomposition analysis for the $F^-(H_2O)_n$ system. (a) OPLS, (b) AMOEBA. Solid lines represent single point values calculated from optimized DFT structures, while the dotted line values were calculated using optimized FF structures.

each table, we provided the energy for each formed dimer calculated using exchange—correlation functionals, the AMOE-BA polarizable force field, and the OPLS and AMBER nonpolarizable force fields, as appropriate. We then compared

the sum of these individual contributions to the total VIE for each of the studied systems.

In Table 4, we show that the total interaction energy in the $NH_3(H_2O)_2$ cluster is -17.18 kcal/mol, while the sum of

Table 3. Correlation Coefficients between Each of the Contributions and the AIE, VIE, and FE for the F⁻(H₂O), System

		AIE		V	TE	FE		
		DFT ^a	FF^{b}	DFT ^a	FF^b	DFT ^a	FF^{b}	
OPLS	bonds	0.073	-0.774	-0.536	-0.809	1.000	0.972	
	angles	-0.632	-0.886	-0.704	-0.912	0.296	0.993	
	vdW	-0.220	-0.778	-0.747	-0.805	0.942	0.908	
	charges	0.482	0.995	0.904	0.999	-0.839	-0.905	
AMOEBA	bonds	-0.406	-0.758	-0.653	-0.763	0.992	0.878	
	angles	-0.892	-0.930	-0.873	-0.931	0.509	0.911	
	UB^c	0.241	0.870	0.189	0.869	0.004	-0.800	
	vdW	-0.588	-0.661	-0.793	-0.667	0.982	0.812	
	PE^d	0.831	0.996	0.955	0.995	-0.897	-0.925	
	Pol. ^e	0.592	0.886	0.792	0.890	-0.971	-0.963	

[&]quot;Single point values calculated over optimized DFT structures. "Values calculated over optimized FF structures. "Urey—Bradley term. "Permanent electrostatic." Polarization.

Table 4. Vertical Interaction Energies and Energy Decomposition Analysis for the NH₃(H₂O)₂ System (Energies in kcal/mol)

				energy decomposition analysis									
	VIE				SAPT(DF	T)		AN	ИОЕВА		OI	PLS	
	ωB97X-D	AMOEBA	OPLS	totala	Elect ^b	$E + I + D^c$	Mult ^d	vdW ^e	Pol ^f	vdW + Pol ^g	q-q ^h	vdW ^e	
						(n = 1)							
NH ₃ -H ₂ O	-7.28	-6.71	-5.94	-5.86	-11.77	5.91	-8.81	4.27	-2.16	2.10	-7.32	1.38	
ÿ 2						(n = 2)							
$NH_3(H_2O)_2$	-17.18	-15.37	-13.88				-19.42	10.87	-6.82	4.05	-18.36	4.48	
$NH_3-H_2O^A$	-3.01	-2.61	-2.74	-2.64	-4.68	2.04	-3.12	1.00	-0.48	0.52	-3.30	0.56	
$NH_3-H_2O^B$	-6.86	-5.72	-5.43	-5.37	-13.67	8.30	-9.66	6.36	-2.41	3.95	-8.05	2.63	
$H_2O^A-H_2O^B$	-4.86	-4.53	-5.72	-3.78	-9.56	5.78	-6.63	3.51	-1.42	2.09	-7.01	1.29	
sum ⁱ	-14.74	-12.86	-13.88	-11.79	-27.91	16.12	-19.42	10.87	-4.31	6.56	-18.36	4.48	
						(n = 3)							
$NH_3(H_2O)_3$	-29.07	-26.80	-24.97				-33.25	20.87	-14.41	6.45	-32.38	7.41	
$NH_3-H_2O^A$	-1.70	-1.47	-1.47	-1.62	-1.42	-0.20	-1.23	-0.17	-0.06	-0.24	-1.33	-0.14	
$NH_3-H_2O^B$	-2.37	-2.02	-3.14	-1.79	-6.04	4.26	-3.60	2.45	-0.86	1.58	-3.98	0.84	
$NH_3-H_2O^C$	-7.17	-5.90	-5.96	-5.57	-15.83	10.27	-11.30	8.19	-2.79	5.40	-9.08	3.11	
$H_2O^A-H_2O^B$	-4.99	-4.74	-6.42	-3.72	-11.20	7.47	-7.75	4.82	-1.81	3.01	-8.08	1.66	
$H_2O^A-H_2O^C$	-4.80	-4.45	-6.55	-3.46	-12.12	8.65	-8.21	5.71	-1.94	3.76	-8.60	2.05	
$H_2O^B-H_2O^C$	-1.52	-1.32	-1.42	-1.43	-1.26	-7.75	-1.15	-0.12	-0.04	-0.17	-1.31	-0.11	
sum ⁱ	-22.55	-19.90	-24.97	-17.59	-47.87	22.70	-33.25	20.87	-7.51	13.35	-32.38	7.41	
						(n = 4)							
$NH_3(H_2O)_4$	-38.89	-35.92	-33.78				-42.72	24.89	-18.09	6.80	-43.08	9.30	
$NH_3-H_2O^A$	-6.10	-5.48	-5.52	-4.59	-12.84	8.25	-8.73	5.53	-2.29	3.25	-7.69	2.16	
$NH_3-H_2O^B$	-1.57	-1.37	-1.53	-1.49	-1.31	-0.18	-1.14	-0.17	-0.06	-0.22	-1.39	-0.14	
$NH_3-H_2O^C$	-2.37	-2.07	-2.10	-2.09	-3.84	1.76	-2.49	0.94	-0.52	0.42	-2.51	0.40	
$NH_3-H_2O^D$	0.34	0.48	1.15	0.44	0.66	-0.22	0.83	-0.24	-0.11	-0.35	1.21	-0.06	
$H_2O^A-H_2O^B$	-4.15	-3.84	-5.78	-2.59	-13.53	10.94	-8.70	6.89	-2.03	4.86	-8.36	2.58	
$H_2O^A-H_2O^C$	-2.21	-1.95	-2.54	-2.08	-1.94	-0.13	-1.68	-0.21	-0.07	-0.28	-2.39	-0.15	
$H_2O^A-H_2O^D$	-3.95	-4.01	-5.13	-3.04	-7.53	4.48	-4.92	1.92	-1.01	0.91	-5.95	0.82	
$H_2O^B-H_2O^C$	-4.37	-3.73	-6.10	-3.02	-12.39	9.37	-8.30	6.60	-2.03	4.57	-8.63	2.53	
H_2O^B - H_2O^D	-1.73	-1.52	-1.93	-1.62	-1.43	-0.18	-1.33	-0.14	-0.05	-0.19	-1.81	-0.12	
$H_2O^C-H_2O^D$	-4.41	-4.11	-4.30	-3.33	-9.17	5.84	-6.27	3.76	-1.60	2.16	-5.58	1.28	
sum ⁱ	-30.51	-27.59	-33.78	-23.41	-63.32	39.91	-42.72	24.89	-9.75	15.14	-43.08	9.30	

 a Total SAPT(DFT). b Electrostatics. c Exchange + induction + dispersion. d Atomic multipole interactions. e van der Waals. f Polarization. g van der Waals + polarization. h Charge—charge interactions. i Sum of pairwise interactions.

pairwise interactions is $-14.74~\rm kcal/mol$ using the $\omega B97X\text{-}D/$ aug-cc-pVDZ level of theory, resulting in an absolute cooperativity of $-2.44~\rm kcal/mol$. Interestingly, using the AMOEBA force field, a cooperativity of $-2.51~\rm kcal/mol$ is observed. Similarly, for the NH $_3(\rm H_2O)_3$ cluster, we calculated an absolute cooperativity of $-6.52~\rm kcal/mol$ and $-6.9~\rm kcal/mol$ using the $\omega B97X\text{-}D/\rm aug\text{-}cc\text{-}pVDZ$ level of theory and the

AMOEBA force field, respectively. For NH₃(H₂O)₄, the calculated absolute cooperativity was -8.38 and -8.33 kcal/mol using the ω B97X-D/aug-cc-pVDZ level of theory and the AMOEBA force field, respectively. Conversely, as expected, the OPLS force field showed no difference between the total interaction energy and the sum of individual interactions.

Table 5. Vertical Interaction Energies and Energy Decomposition Analysis for the Li⁺(H₂O)_n System (Energies in kcal/mol)

				energy decomposition analysis								
		VIE			SAPT(DFT	')		AM	IOEBA		AMB	ER
	M06-2X	AMOEBA	AMBER	total ^a	Elect ^b	$E + I + D^c$	Mult ^d	vdW ^e	Pol ^f	vdW + Pol ^g	q-q ^h	vdW ^e
						(n = 1)						
Li ⁺ -H ₂ O	-36.99	-35.21	-29.88	-32.09	-33.08	0.99	-33.27	12.30	-14.25	-1.95	-41.69	11.81
						(n = 2)						
$Li^+(H_2O)_2$	-69.02	-64.63	-59.28				-63.01	21.50	-23.12	-1.61	-78.40	19.12
Li+-H2OA	-36.94	-34.87	-30.82	-32.08	-32.18	0.10	-32.29	10.81	-13.39	-2.58	-40.45	9.63
Li ⁺ -H ₂ O ^B	-36.94	-34.87	-30.82	-32.21	-32.18	-0.03	-32.29	10.81	-13.39	-2.58	-40.45	9.63
$H_2O^A-H_2O^B$	1.82	1.39	2.36	1.35	1.51	-0.16	1.56	-0.12	-0.06	-0.18	2.50	-0.14
sum ⁱ	-72.05	-68.36	-59.28	-62.94	-62.85	-0.10	-63.01	21.50	-26.85	-5.35	-78.40	19.12
						(n=3)						
$Li^+(H_2O)_3$	-94.70	-86.11	-84.17				-88.81	29.01	-26.31	2.70	-108.87	24.70
Li ⁺ -H ₂ O ^A	-36.84	-34.55	-31.21	-32.26	-31.57	-0.69	-31.57	9.84	-12.82	-2.98	-39.54	8.32
Li+-H ₂ O ^B	-36.84	-34.55	-31.21	-32.15	-31.57	-0.58	-31.57	9.84	-12.82	-2.98	-39.54	8.32
Li ⁺ -H ₂ O ^C	-36.84	-34.54	-31.21	-32.25	-31.57	-0.68	-31.56	9.83	-12.81	-2.98	-39.53	8.32
$H_2O^A-H_2O^B$	2.08	1.68	3.15	1.69	1.73	-0.04	1.96	-0.17	-0.11	-0.28	3.24	-0.09
$H_2O^A-H_2O^C$	2.08	1.69	3.16	1.70	1.73	-0.03	1.96	-0.17	-0.11	-0.28	3.25	-0.09
$H_2O^B-H_2O^C$	2.08	1.69	3.17	1.70	1.73	-0.03	1.97	-0.17	-0.11	-0.28	3.26	-0.09
sum ⁱ	-104.28	-98.58	-84.17	-91.57	-89.52	-2.06	-88.81	29.01	-38.77	-9.76	-108.87	24.70
						(n = 4)						
$Li^{+}(H_2O)_4$	-114.43	-100.90	-103.23				-109.27	33.65	-25.28	8.37	-131.12	27.89
Li ⁺ -H ₂ O ^A	-36.41	-33.94	-31.27	-31.97	-30.62	-1.35	-30.52	8.71	-12.13	-3.42	-38.17	6.90
Li ⁺ -H ₂ O ^B	-36.42	-33.95	-31.28	-31.87	-30.63	-1.23	-30.53	8.72	-12.14	-3.42	-38.19	6.91
Li ⁺ -H ₂ O ^C	-35.92	-33.32	-30.91	-31.51	-29.94	-1.57	-29.80	8.49	-12.01	-3.52	-37.54	6.64
Li ⁺ -H ₂ O ^D	-36.18	-33.78	-30.89	-31.79	-30.47	-1.31	-30.18	8.25	-11.85	-3.60	-37.25	6.36
$H_2O^A-H_2O^B$	2.37	1.75	2.83	1.88	1.96	-0.08	2.00	-0.16	-0.09	-0.25	2.97	-0.14
$H_2O^A-H_2O^C$	1.93	1.75	3.62	1.81	1.49	0.32	2.00	-0.11	-0.15	-0.26	3.46	0.16
H_2O^A - H_2O^D	2.09	1.78	3.45	1.89	1.63	0.26	2.05	-0.13	-0.14	-0.28	3.38	0.07
$H_2O^B-H_2O^C$	1.94	1.75	3.61	1.81	1.50	0.31	2.01	-0.11	-0.15	-0.26	3.46	0.15
H_2O^B - H_2O^D	2.10	1.78	3.45	1.90	1.64	0.26	2.06	-0.14	-0.14	-0.28	3.38	0.06
$H_2O^C-H_2O^D$	1.27	1.55	4.16	1.52	0.62	0.91	1.63	0.14	-0.22	-0.08	3.39	0.77
sum ⁱ	-133.24	-124.63	-103.23	-116.31	-112.83	-3.49	-109.27	33.65	-49.01	-15.37	-131.12	27.89

^aTotal SAPT(DFT). ^bElectrostatics. ^cExchange + induction + dispersion. ^dAtomic multipole interactions. ^evan der Waals. ^fPolarization. ^gvan der Waals + polarization. ^hCharge-charge interactions. ⁱSum of pairwise interactions.

By separating the AMOEBA intermolecular interaction energy into atomic multipoles, van der Waals, and polarization contributions, we can see that the absolute cooperativity arises only from polarization. This is because both the interaction between atomic multipoles and van der Waals interactions are the same in both the cluster and the sum of pairwise interactions. To verify the accuracy of the intermolecular interaction calculations, we compared the electrostatic energy of SAPT(DFT) with the interaction of atomic multipoles or charge-charge interactions for the AMOEBA and OPLS force fields, respectively. Since Psi4 only allows for SAPT(DFT) calculations for dimers, we compute these quantities for every possible dimer in the same first four clusters. The contributions of exchange, induction, and dispersion are compared with the van der Waals interactions and, in the case of AMOEBA, with the sum of van der Waals and polarization. For both the AMOEBA and OPLS force fields, the errors in the electrostatic interaction energy and van der Waals interactions or van der Waals plus polarization in the case of AMOEBA, increase as the system size grows. Both contributions are underestimated, with some canceling each other out. However, the average deviation per dimer is around +3 and -3 kcal/mol for the electrostatic and van der Waals interactions, respectively.

In Table 5, we present the vertical interaction energies per dimer for the $Li^+(H_2O)_n$ system. We calculated an absolute

cooperativity of +3.03 kcal/mol for the Li⁺(H₂O)₂ cluster using the M06-2X/6-311+G(d,p) level of theory. This positive value indicates that the sum of the pairwise interactions is more stable than the total VIE in the cluster. Therefore, it represents a negative cooperativity. With the AMOEBA force field, we observed a negative cooperativity of 3.73 kcal/mol. For the Li⁺(H₂O)₃ and Li⁺(H₂O)₄ systems, we calculated negative cooperativity values of 9.58 and 18.81 kcal/mol using the M06-2X/6-311+G(d,p) level of theory and 12.47 and 23.73 kcal/mol with the AMOEBA force field, respectively. As we can see, the AMOEBA force field successfully predicts the behavior obtained from the electronic structure calculations, although it overestimates negative cooperativity. In the separation of the VIE, the results indicate that the difference in energy arises exclusively from polarization. On the other hand, as expected, the AMBER force field did not exhibit any energy change when calculating the total interactions in the cluster or considering pairwise interactions.

The comparison of electrostatic interactions between the force fields and SAPT(DFT) reveals deviations of less than 1 kcal/mol per dimer for the AMOEBA force field but deviations of up to -8.6 kcal/mol for the AMBER force field in the smallest cluster. The comparison of the sum of exchange, induction, and dispersion with van der Waals plus polarization (for AMOEBA) shows deviations smaller than -3 kcal/mol. In

Table 6. Vertical Interaction Energies and Energy Decomposition Analysis for the F⁻(H₂O)_n System (Energies in kcal/mol)

				energy decomposition analysis									
		VIE			SAPT	Γ(DFT)			AMOEB	SA.	OP	PLS	
	B3LYP	AMOEBA	OPLS	totala	Elect ^b	$E + I + D^c$	Mult^d	vdW ^e	Pol ^f	vdW + Pol ^g	q-q ^h	vdW ^e	
						(n = 1)							
FH ₂ O	-31.56	-22.91	-20.01	-28.59	-43.78	15.18	-34.75	30.78	-18.94	11.84	-35.56	15.54	
2						(n = 2)							
$F^{-}(H_{2}O)_{2}$	-51.41	-45.75	-38.93				-58.06	39.14	-26.83	12.31	-59.31	20.38	
F^- - H_2O^A	-28.47	-27.19	-20.20	-25.69	-36.38	10.69	-29.60	19.62	-17.21	2.41	-30.42	10.23	
$F^H_2O^B$	-28.47	-27.19	-20.19	-25.69	-36.38	10.69	-29.60	19.62	-17.21	2.41	-30.42	10.23	
$H_2O^A-H_2O^B$	0.93	0.93	1.46	0.84	1.06	-0.22	1.14	-0.11	-0.10	-0.20	1.53	-0.07	
sum ⁱ	-56.01	-53.44	-38.93	-50.53	-71.70	21.17	-58.06	39.14	-34.52	4.61	-59.31	20.38	
						(n = 3)							
$F^{-}(H_2O)_3$	-67.42	-64.40	-57.97				-77.19	42.29	-29.50	12.79	-79.40	21.43	
F^- - H_2O^A	-26.89	-28.30	-20.47	-24.35	-32.25	7.90	-26.73	14.23	-15.80	-1.57	-27.70	7.24	
F^- - H_2O^B	-26.89	-28.30	-20.47	-24.35	-32.25	7.90	-26.73	14.22	-15.80	-1.57	-27.70	7.23	
F^- - H_2O^C	-26.89	-28.30	-20.47	-24.35	-32.25	7.90	-26.73	14.22	-15.80	-1.57	-27.70	7.23	
$H_2O^A-H_2O^B$	0.81	0.77	1.14	0.70	0.93	-0.23	1.00	-0.13	-0.10	-0.23	1.23	-0.09	
$H_2O^A-H_2O^C$	0.81	0.77	1.14	0.70	0.93	-0.23	1.00	-0.13	-0.10	-0.23	1.23	-0.09	
$H_2O^B-H_2O^C$	0.81	0.77	1.14	0.70	0.93	-0.23	1.00	-0.13	-0.10	-0.23	1.23	-0.09	
sum ⁱ	-78.23	-82.59	-57.97	-70.94	-93.97	23.03	-77.19	42.29	-47.69	-5.40	-79.40	21.43	
						(n=4)							
$F^{-}(H_2O)_4$	-80.74	-80.00	-77.57				-93.12	40.83	-27.71	13.11	-97.85	20.28	
F^- - H_2O^A	-25.95	-28.08	-19.87	-23.52	-30.25	6.73	-25.23	12.27	-15.12	-2.86	-26.05	6.18	
F^- - H_2O^B	-25.95	-28.08	-19.87	-23.52	-30.25	6.73	-25.23	12.27	-15.12	-2.86	-26.05	6.18	
F^- - H_2O^C	-24.85	-28.06	-21.35	-22.77	-27.70	4.93	-23.25	8.42	-13.23	-4.80	-25.50	4.16	
F^- - H_2O^D	-24.85	-28.06	-21.35	-22.77	-27.70	4.93	-23.25	8.42	-13.23	-4.80	-25.50	4.16	
$H_2O^A-H_2O^B$	0.96	0.96	1.07	0.90	1.04	-0.14	1.08	-0.06	-0.06	-0.11	1.11	-0.04	
$H_2O^A-H_2O^C$	0.00	-0.51	0.25	-0.10	-0.86	0.76	-0.08	-0.15	-0.29	-0.44	0.35	-0.10	
$H_2O^A-H_2O^D$	0.82	0.81	1.04	0.76	0.91	-0.16	0.94	-0.07	-0.06	-0.13	1.09	-0.05	
$H_2O^B-H_2O^C$	0.82	0.81	1.04	0.76	0.91	-0.16	0.94	-0.07	-0.06	-0.13	1.09	-0.05	
H_2O^B - H_2O^D	0.00	-0.51	0.25	-0.10	-0.86	0.76	-0.08	-0.15	-0.29	-0.44	0.35	-0.10	
H_2O^C - H_2O^D	0.93	0.94	1.21	0.87	1.00	-0.13	1.04	-0.05	-0.05	-0.10	1.26	-0.04	
sum ⁱ	-98.07	-109.78	-77.57	-89.50	-113.75	24.25	-93.12	40.83	-57.49	-16.66	-97.85	20.28	

^aTotal SAPT(DFT). ^bElectrostatics. ^cExchange + induction + dispersion. ^dAtomic multipole interactions. ^evan der Waals. ^fPolarization. ^gvan der Waals + polarization. ^hCharge—charge interactions. ⁱSum of pairwise interactions.

the case of AMBER, the deviations reached up to 10.8 kcal/mol for the smallest cluster. These results demonstrate that the error compensation between electrostatic interactions and van der Waals contributions is more pronounced with the AMBER force field.

In Table 6, we present the vertical interaction energies of the $F^{-}(H_2O)_n$ system. Using the B3LYP/aug-cc-pVTZ level of theory, we calculated a negative cooperativity of 4.6 kcal/mol for the $F^-(H_2O)_2$ cluster, 10.81 kcal/mol for the $F^-(H_2O)_3$ cluster, and 17.33 kcal/mol for the F⁻(H₂O)₄ cluster. In contrast, with the AMOEBA force field, we obtained negative cooperativities of 7.69, 18.19, and 29.78 kcal/mol for the $F^{-}(H_2O)_2$, $F^{-}(H_2O)_3$, and $F^{-}(H_2O)_4$ systems, respectively. Once again, with the OPLS force field, there is no difference between the total vertical interaction calculated in the cluster and the sum of pairwise interactions. Upon reviewing the changes in the different contributions to the VIE, we conclude that polarization effects are necessary to reproduce the absolute cooperativity in force fields. This is because they depend on the entire system and cannot be accurately estimated by considering pairwise interactions alone.

When we examine the separation of intermolecular interaction energies into their respective contributions for each dimer and compare them to the results obtained using

SAPT(DFT), it becomes evident that the AMOEBA and OPLS force fields fail to accurately describe the electrostatic interactions. Specifically, deviations of 9.0 and 8.2 kcal/mol are observed for the F^- - H_2O cluster when the AMOEBA and OPLS force fields, respectively. However, these deviations per dimer decrease as the cluster size increases. Surprisingly, the OPLS force field displays remarkable accuracy in representing van der Waals interactions, with deviations of less than 1 kcal/mol for all the studied dimers. Conversely, the AMOEBA force field exhibits significant deviations, reaching up to -8.3 kcal/mol per building block for the $F^-(H_2O)_2$ system.

In order to demonstrate the efficacy of error compensation in obtaining accurate energetics, we performed calculations to assess the errors in adiabatic interaction energies and frustration energies for each cluster (Figures S7–S9). We then computed trend lines in the form of y = mx + b equations and utilized these equations to correct the errors in each cluster (see Figure 6). Our results illustrate that the corrected adiabatic interaction energies exhibit a much-improved performance in reproducing the curves obtained through electronic structure methods.

The interaction energy differences between the classical and quantum representations arise from the limitation of force fields to accurately describe many-body effects. 55 Force fields

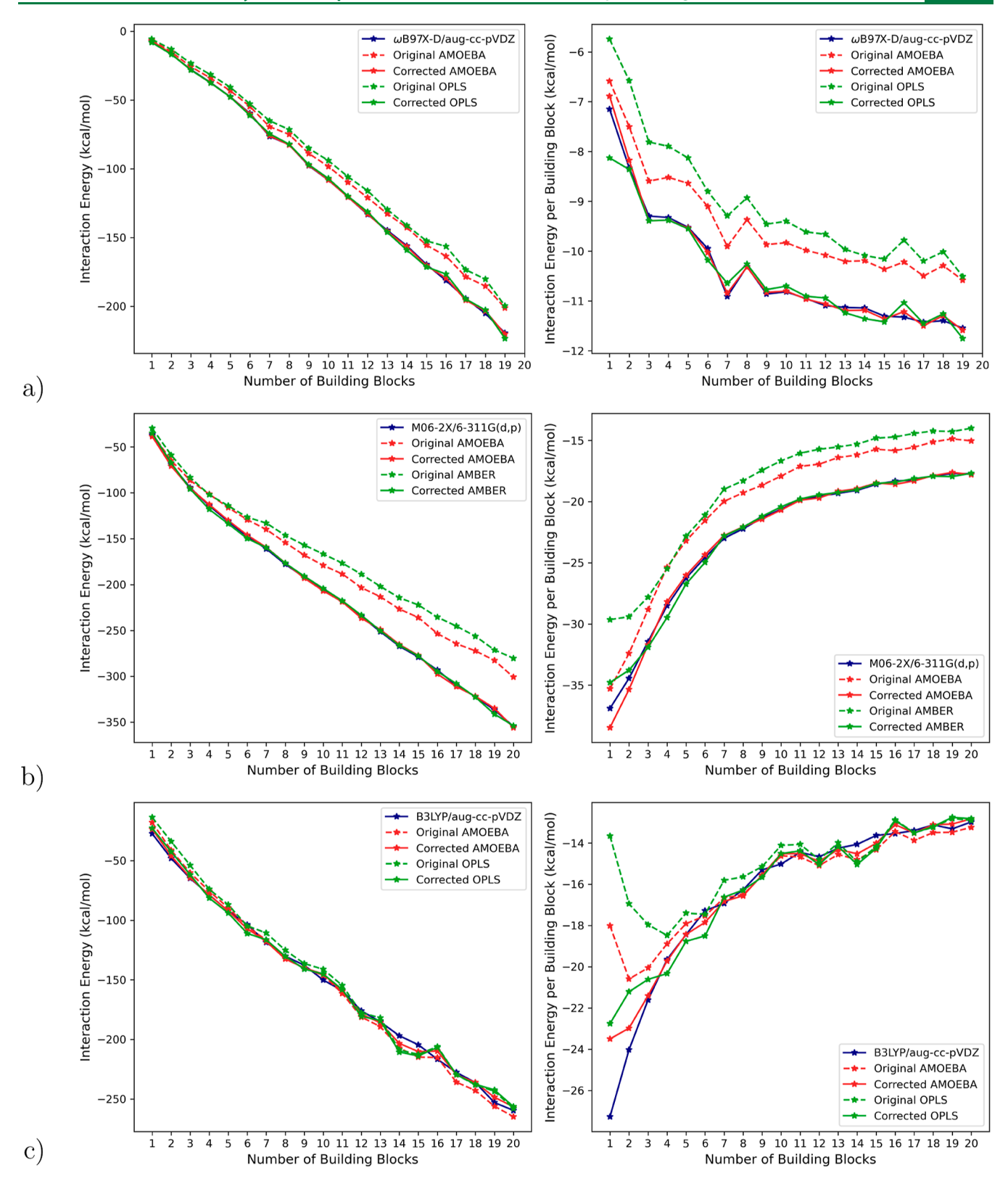


Figure 6. Corrected interaction energies for: (a) $NH_3(H_2O)_n$ system. y = 1.044x - 0.743 and y = 1.181x + 1.202 were used to correct the adiabatic interaction energies for the AMOEBA and OPLS force fields, respectively. (b) $Li^+(H_2O)_n$ system. y = 2.725x + 0.448 and y = 3.600x + 1.535 have been used to correct the adiabatic interaction energies for the AMOEBA and AMBER force fields, respectively. (c) $F^-(H_2O)_n$ system. y = -0.724x + 6.217 and y = -0.564x + 9.661 have been used to correct the adiabatic interaction energies for the AMOEBA and OPLS force fields, respectively.

such as AMBER and OPLS can only explicitly account for oneand two-body contributions and use prepolarized atomcentered charges to reproduce liquid properties (parametrically including some many-body effects). Conversely, AMOEBA

incorporates some approximate many-body contributions by the use of an explicit polarization term. Nevertheless, multipole and van der Waals interactions are still described solely by twobody contributions. Thus, the results presented herein shed light on the drivers of the observed cooperativity effects by classical potentials previously reported in the literature.

CONCLUSIONS

Our findings demonstrate the essential role of polarization effects in qualitatively reproducing what we refer to as absolute cooperativity. This refers to the energy gain or loss observed when calculating the total interaction energy within a given cluster, which cannot be accounted for simply by summing up pairwise interactions. In other words, this requires the calculation of many-body interactions. Specifically, only the AMOEBA polarizable force field was capable of capturing both positive and negative instances of absolute cooperativity. In contrast, the OPLS and AMBER force fields failed to exhibit any form of absolute cooperativity due to their limited consideration of contributions beyond pairwise interactions.

However, in this work, we show that polarizable and nonpolarizable force fields can reproduce the previously examined relative AIE achieved using density functional theory. Our findings suggest that the primary factors responsible for imitating the relative cooperativity are electrostatic interactions. Nevertheless, our results offer valuable insights into the existence of an error compensation mechanism when comparing SAPT(DFT) interaction energies with electrostatic and van der Waals interactions in nonpolarizable force fields or van der Waals interactions combined with polarization in polarizable force fields. The interaction energy errors can be explained in terms of the limitations of force fields in precisely representing the energies involving many-body interactions. Nonpolarizable force fields like AMBER and OPLS only explicitly consider one- and twobody contributions and parametrically include some manybody effects through fitting to bulk properties, while AMOEBA includes some aspects of many-body interactions through polarization. However, multipole and van der Waals interactions in these force fields are still based solely on two-body contributions. The error compensation mechanism provides insights on the reasons why previous studies with nonpolarizable force fields imitate cooperative effects.

On the other hand, frustration is a different phenomenon that arises from alterations in the internal structure of molecules, with the bond stretching term playing the main role in optimized DFT structures and a combination of bond stretching and angle bending terms in optimized FF structures. Our results indicate that whether optimized structures with force fields are used or not has an impact on individual contributions. Our findings can contribute to the development of advanced force fields.

ASSOCIATED CONTENT

Supporting Information

The Supporting Information is available free of charge at https://pubs.acs.org/doi/10.1021/acs.jctc.3c00762.

Single-point and optimized adiabatic and vertical interaction energies, comparison between DFT and force field geometries, root-mean-square deviation for optimize structures, adiabatic interaction and FE errors, and single-point and optimized structures in tinker format (PDF)

Crystallographic coordinates (ZIP)

AUTHOR INFORMATION

Corresponding Author

G. Andrés Cisneros — Department of Physics, University of Texas at Dallas, Richardson, Texas 75080, United States; Department of Chemistry and Biochemistry, University of Texas at Dallas, Richardson, Texas 75080, United States; orcid.org/0000-0001-6629-3430; Email: andres@utdallas.edu

Authors

Jorge Nochebuena — Department of Physics, University of Texas at Dallas, Richardson, Texas 75080, United States; orcid.org/0000-0003-0707-1066

Jean-Philip Piquemal – Laboratoire de Chimie théorique, Sorbonne Université, UMR 7616 CNRS, Paris 75005, France; Oorcid.org/0000-0001-6615-9426

Shubin Liu — Research Computing Center and Department of Chemistry, University of North Carolina, Chapel Hill, North Carolina 27599, United States; orcid.org/0000-0001-9331-0427

Complete contact information is available at: https://pubs.acs.org/10.1021/acs.jctc.3c00762

Notes

The authors declare no competing financial interest.

ACKNOWLEDGMENTS

This work was supported by NIH grant no. R01GM108583. Computational time was provided by the University of North Texas CASCaM CRUNTCh3 high-performance cluster supported by NSF grants no. CHE-1531468 and OAC-2117247.

REFERENCES

- (1) Haino, T. Cooperativity in molecular recognition of feet-to-feet-connected biscavitands. *Pure Appl. Chem.* **2023**, *95*, 343–352.
- (2) Gatto, E.; Toniolo, C.; Venanzi, M. Peptide Self-Assembled Nanostructures: From Models to Therapeutic Peptides. *Nanomaterials* **2022**, *12*, 466.
- (3) Parida, S.; Patra, S. K.; Mishra, S. Self-Assembling Behaviour of Perylene, Perylene Diimide, and Thionated Perylene Diimide Deciphered through Non-Covalent Interactions. *ChemPhysChem* **2022**, 23, No. e202200361.
- (4) Rudharachari Maiyelvaganan, K.; Prakash, M.; Kumar Ravva, M. Simultaneous interaction of graphene nanoflakes with cations and anions: A cooperativity study. *Comput. Theor. Chem.* **2022**, *1209*, 113601.
- (5) Liu, S. Principle of Chirality Hierarchy in Three-Blade Propeller Systems. *J. Phys. Chem. Lett.* **2021**, *12*, 8720–8725.
- (6) Liu, S. Homochirality Originates from the Handedness of Helices. *J. Phys. Chem. Lett.* **2020**, *11*, 8690–8696.
- (7) Yang, X.; Liu, S. Cationic cyclophanes-in-cucurbit[10]uril: host-in-host complexes showing cooperative recognition towards neutral phenol guests. *Supramol. Chem.* **2021**, *33*, 693–700.
- (8) Hu, X.; Liao, M.; Gong, H.; Zhang, L.; Cox, H.; Waigh, T. A.; Lu, J. R. Recent advances in short peptide self-assembly: from rational design to novel applications. *Curr. Opin. Colloid Interface Sci.* **2020**, 45, 1–13
- (9) Li, Y.; Zhao, T.; Wang, C.; Lin, Z.; Huang, G.; Sumer, B. D.; Gao, J. Molecular basis of cooperativity in pH-triggered supramolecular self-assembly. *Nat. Commun.* **2016**, *7*, 13214.
- (10) Mahadevi, A. S.; Sastry, G. N. Cooperativity in Noncovalent Interactions. *Chem. Rev.* **2016**, *116*, 2775–2825.

- (11) Nochebuena, J.; Ireta, J. On cooperative effects and aggregation of GNNQQNY and NNQQNY peptides. *J. Chem. Phys.* **2015**, *143*, 135103.
- (12) Rong, C.; Zhao, D.; He, X.; Liu, S. Development and Applications of the Density-Based Theory of Chemical Reactivity. *J. Phys. Chem. Lett.* **2022**, *13*, 11191–11200.
- (13) Li, Y.; Ji, C.; Xu, W.; Zhang, J. Z. H. Dynamical Stability and Assembly Cooperativity of β -Sheet Amyloid Oligomers Effect of Polarization. *J. Phys. Chem. B* **2012**, *116*, 13368–13373.
- (14) Wu, Y.-D.; Zhao, Y.-L. A Theoretical Study on the Origin of Cooperativity in the Formation of 3_{10} and α -Helices. *J. Am. Chem. Soc.* **2001**, *123*, 5313–5319.
- (15) Piskorz, T. K.; de Vries, A. H.; van Esch, J. H. How the Choice of Force-Field Affects the Stability and Self-Assembly Process of Supramolecular CTA Fibers. *J. Chem. Theory Comput.* **2022**, *18*, 431–440.
- (16) Lemkul, J. A.; Huang, J.; Roux, B.; MacKerell, A. D. An Empirical Polarizable Force Field Based on the Classical Drude Oscillator Model: Development History and Recent Applications. *Chem. Rev.* **2016**, *116*, 4983–5013.
- (17) Vanommeslaeghe, K.; MacKerell, A. CHARMM additive and polarizable force fields for biophysics and computer-aided drug design. *Biochim. Biophys. Acta, Gen. Subj.* **2015**, *1850*, 861–871.
- (18) Huang, J.; MacKerell, A. D. Induction of Peptide Bond Dipoles Drives Cooperative Helix Formation in the (AAQAA)₃ Peptide. *Biophys. J.* **2014**, *107*, 991–997.
- (19) Chen, B.; Xing, J.; Siepmann, J. I. Development of Polarizable Water Force Fields for Phase Equilibrium Calculations. *J. Phys. Chem. B* **2000**, *104*, 2391–2401.
- (20) Penev, E.; Ireta, J.; Shea, J.-E. Energetics of Infinite Homopolypeptide Chains: A New Look at Commonly Used Force Fields. J. Phys. Chem. B 2008, 112, 6872–6877.
- (21) Melcr, J.; Piquemal, J.-P. Accurate Biomolecular Simulations Account for Electronic Polarization. *Front. Mol. Biosci.* **2019**, *6*, 143.
- (22) Ponder, J. W.; Case, D. A. *Protein Simulations*; Advances in Protein Chemistry; Academic Press, 2003; Vol. 66, pp 27–85.
- (23) Rong, C.; Zhao, D.; Yu, D.; Liu, S. Quantification and origin of cooperativity: insights from density functional reactivity theory. *Phys. Chem. Chem. Phys.* **2018**, *20*, 17990–17998.
- (24) Zhou, T.; Liu, S.; Yu, D.; Zhao, D.; Rong, C.; Liu, S. On the negative cooperativity of argon clusters containing one lithium cation or fluorine anion. *Chem. Phys. Lett.* **2019**, *716*, 192–198.
- (25) Rong, C.; Zhao, D.; Zhou, T.; Liu, S.; Yu, D.; Liu, S. Homogeneous Molecular Systems are Positively Cooperative, but Charged Molecular Systems are Negatively Cooperative. *J. Phys. Chem. Lett.* **2019**, *10*, 1716–1721.
- (26) Liu, S.; Rong, C. Quantifying Frustrations for Molecular Complexes with Noncovalent Interactions. *J. Phys. Chem. A* **2021**, 125, 4910–4917.
- (27) Nochebuena, J.; Cuautli, C.; Ireta, J. Origin of cooperativity in hydrogen bonding. *Phys. Chem. Chem. Phys.* **2017**, *19*, 15256–15263.
- (28) Hofer, T. S.; Tran, H. T.; Schwenk, C. F.; Rode, B. M. Characterization of dynamics and reactivities of solvated ions by ab initio simulations. *J. Comput. Chem.* **2004**, *25*, 211–217.
- (29) Tongraar, A.; Rode, B. M. Ab initio QM/MM dynamics of anion—water hydrogen bonds in aqueous solution. *Chem. Phys. Lett.* **2005**, *403*, 314–319.
- (30) Tongraar, A.; Liedl, K. R.; Rode, B. M. The hydration shell structure of Li+ investigated by Born-Oppenheimer ab initio QM/MM dynamics. *Chem. Phys. Lett.* **1998**, 286, 56–64.
- (31) Frisch, M. J. et al. Gaussian 16 Revision C.01. 2016.
- (32) Chai, J.-D.; Head-Gordon, M. Long-range corrected hybrid density functionals with damped atom—atom dispersion corrections. *Phys. Chem. Phys.* **2008**, *10*, 6615–6620.
- (33) Prascher, B. P.; Woon, D. E.; Peterson, K. A.; Dunning, T. H.; Wilson, A. K. Gaussian basis sets for use in correlated molecular calculations. VII. Valence, core-valence, and scalar relativistic basis sets for Li, Be, Na, and Mg. *Theor. Chem. Acc.* **2011**, *128*, 69–82.

- (34) Dunning, T. H. Gaussian basis sets for use in correlated molecular calculations. I. The atoms boron through neon and hydrogen. *J. Chem. Phys.* **1989**, *90*, 1007–1023.
- (35) Kendall, R. A.; Dunning, T. H.; Harrison, R. J. Electron affinities of the first?row atoms revisited. Systematic basis sets and wave functions. *J. Chem. Phys.* **1992**, *96*, 6796–6806.
- (36) Zhao, Y.; Truhlar, D. G. The M06 suite of density functionals for main group thermochemistry, thermochemical kinetics, non-covalent interactions, excited states, and transition elements: two new functionals and systematic testing of four M06-class functionals and 12 other functionals. *Theor. Chem. Acc.* 2008, 120, 215–241.
- (37) Clark, T.; Chandrasekhar, J.; Spitznagel, G. W.; Schleyer, P. V. R. Efficient diffuse function-augmented basis sets for anion calculations. III. The 3-21+G basis set for first-row elements, Li–F. *J. Comput. Chem.* 1983, 4, 294–301.
- (38) Krishnan, R.; Binkley, J. S.; Seeger, R.; Pople, J. A. Self-consistent molecular orbital methods. XX. A basis set for correlated wave functions. *J. Chem. Phys.* **1980**, *72*, 650–654.
- (39) Shi, Y.; Xia, Z.; Zhang, J.; Best, R.; Wu, C.; Ponder, J. W.; Ren, P. Polarizable Atomic Multipole-Based AMOEBA Force Field for Proteins. *J. Chem. Theory Comput.* **2013**, *9*, 4046–4063.
- (40) Zhang, C.; Lu, C.; Jing, Z.; Wu, C.; Piquemal, J.-P.; Ponder, J. W.; Ren, P. AMOEBA Polarizable Atomic Multipole Force Field for Nucleic Acids. *J. Chem. Theory Comput.* **2018**, *14*, 2084–2108.
- (41) Becke, A. D. Density-functional thermochemistry. III. The role of exact exchange. *J. Chem. Phys.* **1993**, *98*, 5648–5652.
- (42) Lee, C.; Yang, W.; Parr, R. G. Development of the Colle-Salvetti correlation-energy formula into a functional of the electron density. *Phys. Rev. B: Condens. Matter Mater. Phys.* **1988**, 37, 785–789.
- (43) Ren, P.; Wu, C.; Ponder, J. W. Polarizable Atomic Multipole-based Molecular Mechanics for Organic Molecules. *J. Chem. Theory Comput.* **2011**, *7*, 3143–3161.
- (44) Ren, P.; Ponder, J. W. Polarizable Atomic Multipole Water Model for Molecular Mechanics Simulation. *J. Phys. Chem. B* **2003**, 107, 5933–5947.
- (45) Ren, P.; Ponder, J. W. Consistent treatment of inter- and intramolecular polarization in molecular mechanics calculations. *J. Comput. Chem.* **2002**, 23, 1497–1506.
- (46) Kaminski, G. A.; Friesner, R. A.; Tirado-Rives, J.; Jorgensen, W. L. Evaluation and Reparametrization of the OPLS-AA Force Field for Proteins via Comparison with Accurate Quantum Chemical Calculations on Peptides. *J. Phys. Chem. B* **2001**, *105*, 6474–6487.
- (47) Maier, J. A.; Martinez, C.; Kasavajhala, K.; Wickstrom, L.; Hauser, K. E.; Simmerling, C. ff14SB: Improving the Accuracy of Protein Side Chain and Backbone Parameters from ff99SB. *J. Chem. Theory Comput.* **2015**, *11*, 3696–3713.
- (48) Rackers, J. A.; Wang, Z.; Lu, C.; Laury, M. L.; Lagardère, L.; Schnieders, M. J.; Piquemal, J.-P.; Ren, P.; Ponder, J. W. Tinker 8: Software Tools for Molecular Design. *J. Chem. Theory Comput.* **2018**, 14, 5273–5289.
- (49) Jorgensen, W. L.; Chandrasekhar, J.; Madura, J. D.; Impey, R. W.; Klein, M. L. Comparison of simple potential functions for simulating liquid water. *J. Chem. Phys.* **1983**, *79*, 926–935.
- (50) Dang, L. X.; Pettitt, B. M. Simple intramolecular model potentials for water. *J. Phys. Chem.* **1987**, *91*, 3349–3354.
- (51) Halgren, T. A. The representation of van der Waals (vdW) interactions in molecular mechanics force fields: potential form, combination rules, and vdW parameters. *J. Am. Chem. Soc.* **1992**, *114*, 7827–7843.
- (52) Jorgensen, W. L.; Maxwell, D. S.; Tirado-Rives, J. Development and Testing of the OPLS All-Atom Force Field on Conformational Energetics and Properties of Organic Liquids. *J. Am. Chem. Soc.* **1996**, *118*, 11225–11236.
- (53) Weiner, S. J.; Kollman, P. A.; Case, D. A.; Singh, U. C.; Ghio, C.; Alagona, G.; Profeta, S.; Weiner, P. A new force field for molecular mechanical simulation of nucleic acids and proteins. *J. Am. Chem. Soc.* 1984, 106, 765–784.

- (54) Weiner, S. J.; Kollman, P. A.; Nguyen, D. T.; Case, D. A. An all atom force field for simulations of proteins and nucleic acids. *J. Comput. Chem.* **1986**, *7*, 230–252.
- (55) Hankins, D.; Moskowitz, J. W.; Stillinger, F. H. Water Molecule Interactions. *J. Chem. Phys.* **1970**, *53*, 4544–4554.